

NaviDriveVLM: Decoupling High-Level Reasoning and Motion Planning for Autonomous Driving

Ximeng Tao¹, Pardis Taghavi¹, Dimitar Filev¹, Reza Langari¹, Gaurav Pandey²

Abstract—Vision-language models (VLMs) have emerged as a promising direction for end-to-end autonomous driving (AD) by jointly modeling visual observations, driving context, and language-based reasoning. However, existing VLM-based systems face a trade-off between high-level reasoning and motion planning: large models offer strong semantic understanding but are costly to adapt for precise control, whereas small VLM models can be fine-tuned efficiently but often exhibit weaker reasoning. We propose NaviDriveVLM, a decoupled framework that separates reasoning from action generation using a large-scale Navigator and a lightweight trainable Driver. This design preserves reasoning ability, reduces training cost, and provides an explicit interpretable intermediate representation for downstream planning. Experiments on the nuScenes benchmark show that NaviDriveVLM outperforms large VLM baselines in end-to-end motion planning. Codes are available at: <https://github.com/TAMU-CVRL/NaviDrive>.

I. INTRODUCTION

End-to-end autonomous driving (AD) has evolved from systems focused primarily on perception [1] to frameworks that must jointly understand scene context, follow navigation intent, and generate reliable future actions [2], [3]. In parallel, recent advances that incorporate language have opened a promising direction for AD by combining visual perception with semantic reasoning and language-guided decision making. Early efforts explored language-based decision making for driving [4], while subsequent vision-language and vision-language-action models further unified perception, reasoning, and trajectory generation within a single architecture [5], [6], [7], [8], [9], [10]. More recent systems continue to strengthen this trend through improved reasoning quality, action generation, and multimodal specialization [11], [12], [13]. Compared with conventional modular systems, these models offer the appealing possibility of improved interpretability, since they can explicitly describe traffic scenes, justify decisions, and expose intermediate reasoning. Such properties are particularly valuable in safety critical driving, where transparent decision making is as important as planning accuracy.

However, existing VLM-based driving systems still face a basic trade-off between high-level reasoning and motion planning. Larger models are often better at understanding the scene and semantic reasoning, but they are not naturally

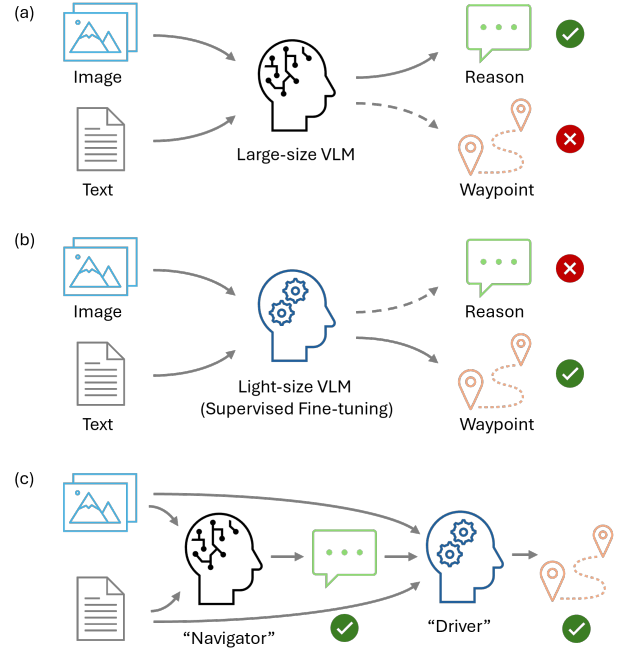


Fig. 1. (a) Large-scale VLMs show strong reasoning ability but fail to generate accurate driving actions without fine-tuning. (b) Lightweight VLMs can be fine-tuned for future waypoints prediction, but their reasoning ability degrades. (c) We decouple reasoning and motion planning into two modules, using a large-scale VLM as the Navigator for reasoning and a lightweight VLM as the Driver for waypoint prediction, preserving reasoning while optimizing driving performance.

optimized for precise motion prediction or direct action generation without costly task-specific adaptation [8], [9], [10]. In contrast, smaller models can be fine-tuned more efficiently for waypoint or action prediction, but they often need extra supervision, reasoning transfer, or distillation to recover the benefits of stronger semantic guidance [14], [15], [16], [17], [12]. As a result, using a single model to jointly perform reasoning and control can lead to a difficult balance between reasoning quality, adaptation efficiency, and planning accuracy.

To address this challenge, we propose **NaviDriveVLM**, a decoupled framework that separates semantic reasoning from action generation. It consists of a frozen large-scale VLM, referred to as the *Navigator*, and a lightweight trainable VLM, referred to as the *Driver*. The Navigator takes surround view images, ego states, and task prompts as input, and produces semantic guidance in the form of a scene description, a recommended action, and the corresponding reasoning. The Driver then uses this reasoning output, images, ego states,

¹Ximeng Tao, Pardis Taghavi, Dimitar Filev and Reza Langari are with J. Mike Walker '66 Department of Mechanical Engineering, Texas A&M University, College Station, TX 77843, USA ximeng, ptgh, dfilev, rlangari@tamu.edu

²Gaurav Pandey is with The Department of Engineering Technology and Industrial Distribution Texas A&M University, College Station, TX 77843, USA gpandey@tamu.edu

and task prompts to predict future waypoints. Keeping the Navigator frozen preserves strong reasoning ability while avoiding the computational burden of retraining a large model. The specialized Driver can be adapted efficiently for downstream motion prediction. This design turns semantic reasoning into an explicit and interpretable intermediate representation between perception and planning.

We evaluate NaviDriveVLM for end-to-end motion planning task on the nuScenes benchmark [18]. Our results show that the decoupled design outperforms single large-VLM baselines that directly fine-tune a standalone model for trajectory prediction, and our ablations further show that the Navigator’s reasoning improves planning performance. Together, these findings indicate that separating semantic reasoning from motion planning is a useful design choice for building VLM-based AD systems that are both more interpretable and more effective.

Our contributions are threefold: 1) we introduce NaviDriveVLM, a decoupled Navigator–Driver framework for autonomous driving; 2) we show that structured reasoning can serve as an interpretable intermediate representation for improving waypoint prediction; and 3) we evaluate NaviDriveVLM on the nuScenes benchmark and show that the decoupled design achieves stronger planning performance than single large-VLM baselines, while retaining interpretability and reducing adaptation cost.

II. RELATED WORK

A. VLMs for End-to-End Autonomous Driving

Recent end-to-end driving research has increasingly incorporated language modeling to improve generalization and semantic understanding. Early planning-oriented frameworks such as UniAD [2] unified perception, prediction, and planning toward the final driving objective, while language-driven systems such as GPT-Driver [19], DriveMLM [20], and LMDrive [21] showed that LLMs can support motion planning, behavior planning, and instruction-following driving. More recent multimodal systems, including Driving with LLMs [5], DriveGPT4 [6], EMMA [8], and DriveMoE [10], further integrate visual perception, language reasoning, and trajectory prediction within a single model. Collectively, these works show the promise of VLMs for AD, but most still rely on a unified model to perform both high-level reasoning and future waypoints generation, making it difficult to simultaneously preserve strong reasoning ability, efficient adaptation, and precise control.

B. Semantic Reasoning and Explainability

A parallel line of work uses language to improve interpretability and make driving decisions more transparent. DriveLM [22] explicitly decomposes reasoning across perception, prediction, and planning. Reason2Drive [23] advances this direction with a large-scale benchmark for interpretable, chain-based reasoning in driving scenes, while RAG-Driver [24] improves explanation quality through retrieval augmented reasoning. Related systems such as Alpamayo [11] and DriveGPT4-v2 [13] also generate natural-

language rationales together with actions or decisions. These studies establish language is valuable not only for supervision but also for exposing intermediate decision logic; however, in most prior work, reasoning primarily serves as an auxiliary explanation signal rather than a separated intermediate representation for downstream control.

C. Decoupled and Hierarchical Driving Architectures

Separating high-level decision-making from motion planning is a long-standing principle in autonomous driving, and several recent driving systems adopt modular forms of integration between reasoning and planning. Hydra-MDP [3] uses a teacher-student formulation with multi-target hydra distillation to learn diverse trajectory candidates, while VLM-AD [14] and DiMA [15] leverage VLM/MLLM supervision during training to improve a lighter planner. More recent methods such as DSDrive [17] and LeapVAD [12] further emphasize integration of reasoning and planning through distillation or dual-process design. While recent modular architectures often utilize reasoning as a supervision signal during training, NaviDriveVLM employs reasoning as an explicit and interpretable intermediate representation. By decoupling a frozen, large-scale Navigator from a lightweight, trainable Driver, we preserve complex semantic guidance while achieving precise motion planning.

III. METHODOLOGY

The overall architecture of our framework is shown in Fig. 2. The system is decoupled into two modules, the *Navigator* and the *Driver*. The Navigator is a large-scale VLM responsible for scene understanding and high-level reasoning. In principle, it can be replaced by any advanced reasoning-capable VLM. To preserve its inherent reasoning capability and avoid the substantial computational cost associated with retraining large-scale parameters, the Navigator remains frozen during training. The Driver is a lightweight VLM, which enables efficient fully supervised fine-tuning (SFT) as a driving expert for future waypoint prediction.

A. Navigator

A pretrained large scale VLM is used as a *Navigator* which generates the scene description, action and reasoning for the suggested action. It takes the multi-view surrounding images (\mathcal{I}), the ego-vehicle state ($O_{ego} = [\text{velocity } (v), \text{yaw rate } (r), \text{acceleration } (\alpha)]$), past waypoints (x_t, y_t), and a high-level command as input (Fig. 2). The high-level command is determined based on the ground-truth waypoints and recorded in the training dataset. It categorizes driver intention into six classes: *Hard Left*, *Slight Left*, *Keep Straight*, *Slight Right*, *Hard Right*, and *Decelerate Stop*. The user prompt and system prompt for this Navigator VLM (Navi-VLM) are represented as Q_N and S_N , respectively, with detailed content shown in the upper part of Fig. 3. The Navi-VLM is denoted as \mathcal{G}_N , and the reasoning generation process can be described as:

$$O_R = \mathcal{G}_N(\mathcal{I}, O_{ego}, Q_N, S_N). \quad (1)$$

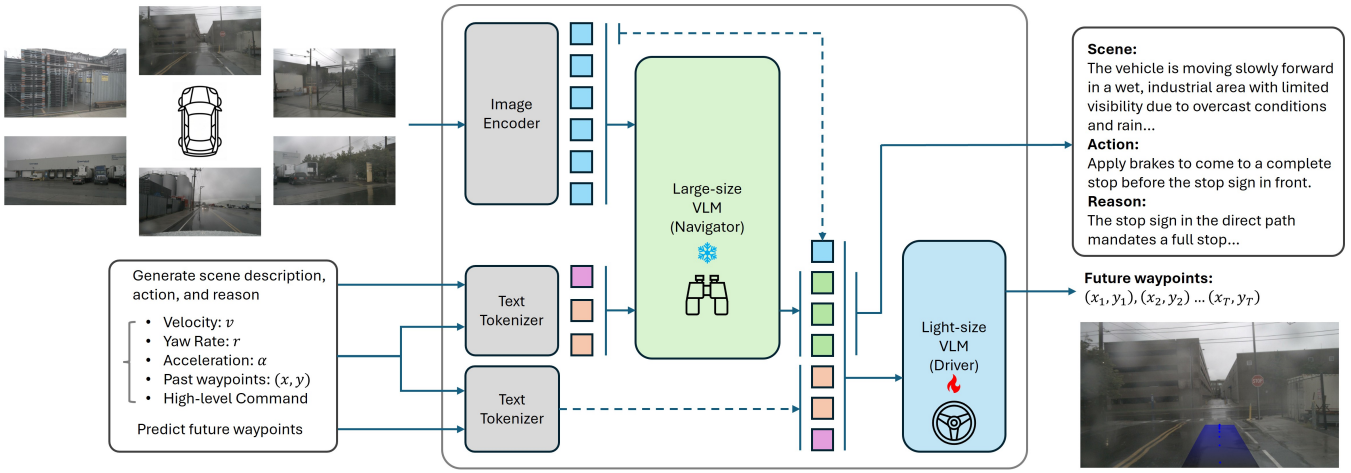


Fig. 2. Overview of NaviDriveVLM. The framework is decoupled into a large VLM serving as the Navigator and a lightweight VLM serving as the Driver. (a) Multi-view surround images are encoded into visual tokens (blue). The Navigator prompt and ego state are tokenized as text tokens (pink and orange). (b) The Navigator VLM generates reasoning tokens (green), which are concatenated with the front-view image tokens, Driver prompt, and ego state tokens, and then fed into the Driver VLM. (c) The Driver VLM is fine-tuned to predict future waypoints or driving actions. The reasoning tokens can be decoded into text for interpretability.

The reasoning output O_R consists of three components: scene description, recommended action, and corresponding reasoning explanation. These reasoning tokens can be directly forwarded to the lightweight Driver VLM (Driver-VLM) to assist future waypoint prediction and improve planning performance, or decoded to obtain human-readable explanations.

B. Driver

A lightweight VLM is fully fine-tuned to serve as a driver expert, enabling it to understand reasoning outputs and observational inputs to predict future waypoints ($\mathcal{W} = \{w_t = (x_t, y_t)\}_{t=1}^T$). In Eq. 2, in addition to the four common inputs ($\mathcal{I}, O_{ego}, Q_D, S_D$), the reasoning output O_R is introduced. The system and user prompts differ from those used in Navi-VLM and are shown in the lower part of Fig. 3. The reasoning output O_R generated by the Navi-VLM is incorporated as an auxiliary input. The reasoning information plays an important role in improving prediction accuracy.

$$\mathcal{W} = \mathcal{G}_D(O_R, \mathcal{I}, O_{ego}, Q_D, S_D). \quad (2)$$

The VLM-based approach models waypoint prediction as a probabilistic generation process, formulated as

$$P(\mathcal{W} | O_R, \mathcal{I}, O_{ego}, Q_D, S_D), \quad (3)$$

where \mathcal{W} denotes the future waypoint sequence. During the SFT stage, we optimize the Driver-VLM parameters θ_D by minimizing the negative log-likelihood of the ground-truth waypoint sequence \mathcal{W} . w_t is the target waypoint to be predicted at frame t , and $w_{<t}$ represent the ground-truth waypoints from previous time steps. The loss function is defined as:

$$\mathcal{L}_{SFT} = - \sum_{t=1}^T \log P(w_t | w_{<t}, O_R, \mathcal{I}, O_{ego}, Q_D, S_D; \theta_D). \quad (4)$$

The ground-truth waypoints are used as assistant prompts during training, and non-target tokens are masked under the autoregressive training objective.

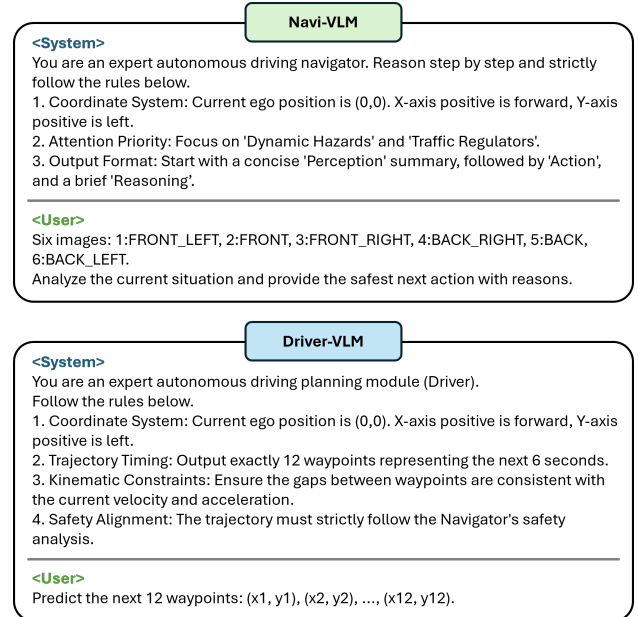


Fig. 3. Prompt design for the Navi-VLM and Driver-VLM.

IV. EXPERIMENTS

A. Dataset

We use the nuScenes dataset [18] to construct a derived dataset, referred to as the nuScenes-Reason dataset. The nuScenes contains 850 scenes, where each scene consists of 20-second driving sequences sampled at 2 Hz. We employ an 8-second sliding window to extract thirteen 8-second

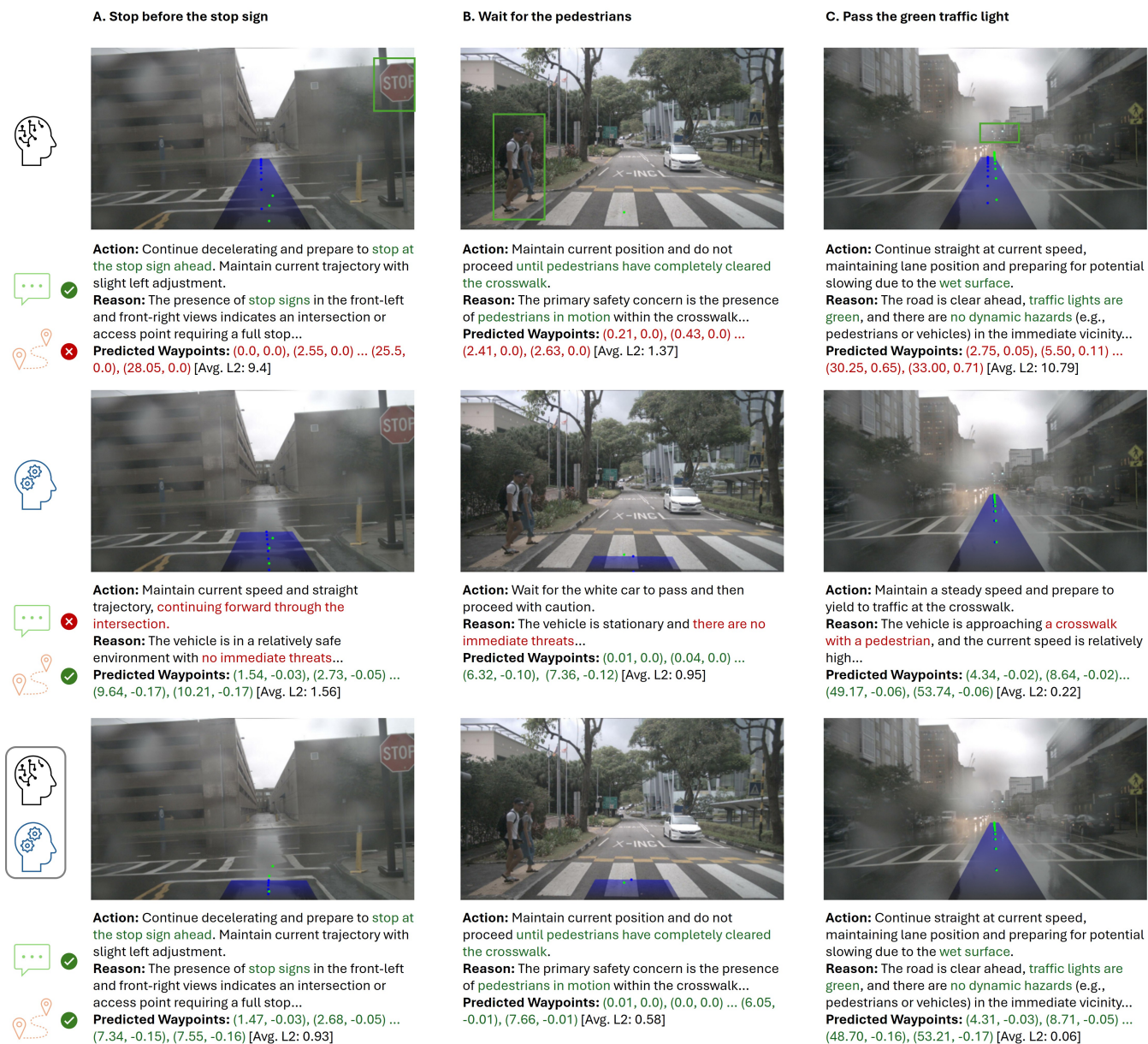


Fig. 4. Qualitative results across three different driving scenarios. Predicted waypoints are visualized as blue masks and blue dots, while ground-truth waypoints are shown in green. The minimum average L2 error in meters over 6 seconds is shown in brackets. The first row represents a non-fine-tuned large VLM, which is capable of generating reasonable high-level reasoning outputs. However, the predicted future waypoints deviate significantly from the ground truth. The second row corresponds to a smaller fine-tuned VLM, which can generate accurate future waypoints suitable for control. However, it lacks strong scene understanding and reasoning capabilities. The third row presents our proposed NaviDriveVLM framework, which combines reliable high-level reasoning with accurate future waypoint prediction.

clips from each scene, which are further divided into a 2-second historical context and a 6-second future prediction horizon. Meanwhile, the waypoints, heading, velocity, yaw rate, acceleration, and images associated with these clips are recorded for further training and evaluation. This procedure yields 16.54k training samples and 3618 test samples. To accelerate the training process, we decouple training into two stages. First, a large pre-trained VLM (NaviVLM) is used to generate reasoning outputs for each 8-second clip. The generated reasoning results are recorded as text, constructing the nuScenes-Reason dataset. Second, Driver-VLM is trained

using the nuScenes-Reason dataset, avoiding repeated NaviVLM inference and improving training efficiency.

B. Training

Qwen3 [31] performs well among open-source VLMs and is therefore adopted as the backbone model for both NaviVLM and Driver-VLM. During training, only the Driver-VLM is fine-tuned using SFT. We employ the AdamW optimizer [32] with a weight decay of 0.01 and an initial learning rate of 1×10^{-5} . A cosine learning rate schedule is adopted. The batch size is set to 1, and the model is

D. Wait for the red traffic light



Action: Maintain current position and remain stopped. Wait for the traffic light to turn green before proceeding.

Reason: The ego vehicle is stationary and aligned with traffic flow, which is halted at a red light...

Predicted Waypoints: (0, 0), (0, 0) ... (0, 0), (0, 0) [Avg. L2: 0.08]

E. Following the vehicle ahead

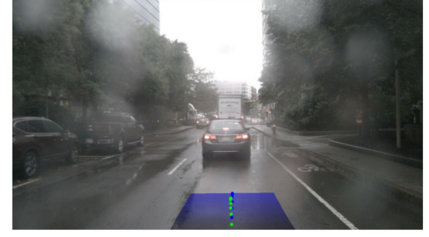


Action: Continue straight ahead at current speed, maintaining lane position, and prepare to follow the white van while maintaining a safe distance.

Reason: The road ahead is clear of dynamic hazards, and no traffic signals or signs require immediate change in direction or speed...

Predicted Waypoints: (4.85, 0.03), (9.75, 0.21) ... (52.22, 6.19), (56.87, 7.21) [Avg. L2: 0.62]

F. Braking



Action: Continue decelerating at a moderate rate and maintain current lane position.

Reason: The vehicle ahead is braking, as indicated by its illuminated brake lights, and the ego-vehicle is already decelerating...

Predicted Waypoints: (1.48, -0.01), (2.67, -0.01) ... (8.36, -0.07), (8.49, -0.07) [Avg. L2: 0.24]

Fig. 5. Additional qualitative results from NaviDriveVLM. Predicted waypoints are visualized as blue masks and blue dots, while ground-truth waypoints are shown in green. The minimum average L2 error in meters over 6 seconds is shown in brackets. Scenes D, E, and F illustrate the reasoning results and the corresponding predicted future waypoints predicted by NaviDriveVLM across three scenarios: waiting at a red traffic light, following another vehicle, and braking.

TABLE I
END-TO-END MOTION PLANNING EXPERIMENTS ON NUSCENES

Model	VLM	L2 (1s)	L2 (2s)	L2 (3s)	Avg. L2 (m) ↓
OpenEMMA [25]	LLaVa-7B [26]	1.45	3.21	3.76	2.81
ST-P3 [27]	-	1.33	2.11	2.90	2.11
GenAD [28]	-	0.36	0.83	1.55	0.91
Ego-MLP [29]	-	0.46	0.76	1.12	0.78
VAD-Base [30]	-	0.41	0.70	1.05	0.72
UniAD [2]	-	0.44	0.67	0.96	0.69
Verdi [16]	-	0.36	0.62	0.96	0.65
Driver-VLM	Qwen3-VL-8B	0.24	0.65	1.25	0.60
NaviDriveVLM	Qwen3-VL-2B	0.20	0.50	0.93	0.46

trained for 3 epochs. Gradient accumulation is performed over 16 steps. For the 8B-scale model, 8-bit quantization and LoRA adaptation [33] are applied, with a LoRA rank of 64, LoRA alpha of 128, and LoRA dropout rate of 0.05. All experiments are conducted on a single NVIDIA RTX 4090 GPU.

C. Metrics

For Navi-VLM, evaluating the correctness of reasoning outputs is inherently subjective and difficult to quantify. Therefore, we primarily rely on the general reasoning capability of modern large-scale VLMs and provide qualitative analysis of representative results in Section IV-D. For the overall NaviDriveVLM framework, we focus on the open-loop motion planning task. The model generates six candidate future waypoints, and the prediction with the smallest minimum Average L2 Error at the 6-second prediction horizon is selected for evaluation.

D. Results

Fig. 4 presents qualitative comparisons across three representative driving scenarios: A) stopping before a stop sign, B) yielding to pedestrians, and C) proceeding through a green traffic light. The first row shows results from a

large VLM without supervised fine-tuning (Qwen3-VL-8B). Although this model produces reasonable semantic reasoning, it predicts inaccurate future waypoints, as reflected by the large average L2 error highlighted in red (First row, Fig. 4). These examples indicate that a pretrained large VLM can recognize important scene elements, such as stop signs, pedestrians in the crosswalk, and traffic light states, but without task-specific adaptation it does not generate reliable motion predictions. The second row shows results from a smaller VLM (Qwen3-VL-2B) after supervised fine-tuning. In this case, waypoint prediction becomes more accurate, but the quality of the reasoning degrades. The incorrect or incomplete reasoning is highlighted in red in the second row of Fig. 4. This suggests that fine-tuning a lightweight model improves prediction, but may weaken its high-level semantic reasoning. The third row presents results from the proposed NaviDriveVLM framework. By decoupling reasoning and control, NaviDriveVLM combines the strong semantic reasoning of a large VLM with the accurate waypoint prediction of a fine-tuned lightweight VLM. As shown in Fig. 4, this design produces both reliable reasoning outputs and trajectories that more closely match the ground truth. Fig. 5 presents additional qualitative results

TABLE II
COMPARISON OF WAYPOINT AND ACTION PREDICTION PERFORMANCE

Model	Output	L2 (1s)	L2 (2s)	L2 (3s)	L2 (6s)	Avg. L2 (m) ↓
NaviDriveVLM	Waypoint (x, y)	0.200	0.495	0.934	3.245	1.285
	Action (α, κ)	0.259	0.571	1.007	2.911	1.201

TABLE III
ABLATION STUDY ON INPUT COMPONENTS OF NAVIDRIVEVLM

Model	Reason	Command	Images	L2 (1s)	L2 (2s)	L2 (3s)	L2 (6s)	Avg. L2 (m) ↓
NaviDriveVLM	✓			0.204	0.518	1.029	3.977	1.515
	✓		✓	0.200	0.516	1.012	3.861	1.476
	✓	✓		0.200	0.496	0.934	3.254	1.288
	✓	✓	✓	0.200	0.495	0.934	3.245	1.285

of our proposed NaviDriveVLM framework across diverse driving scenarios.

In Table I, we report open-loop motion planning results on the nuScenes dataset. At the 3-second horizon (Table I), NaviDriveVLM outperforms several representative prior methods, including ST-P3 [27], Ego-MLP [29], and UniAD [2]. To better isolate the effect of explicit reasoning, we include a Driver-VLM baseline that removes the Navigator and uses a single VLM backbone for trajectory prediction. Compared with OpenEMMA, supervised fine-tuning of this single-model baseline leads to a clear improvement in planning accuracy. Moreover, when the Navigator is added, the performance improves further, showing that explicit semantic guidance contributes beyond supervised fine-tuning alone. Overall, these results highlight the importance of reasoning information in motion planning and support the effectiveness of the proposed decoupled framework for improving prediction performance.

E. Waypoints vs. Control Actions

The NaviDriveVLM is primarily trained to predict future waypoints. Additionally, we investigate an alternative formulation in which the model directly predicts driving actions. Since the nuScenes dataset does not provide control actions as ground-truth labels, we utilize ground-truth waypoints and convert them into corresponding control actions to serve as training supervision. To transform the discrete waypoint sequence into a continuous and kinematically feasible control sequence \mathbf{u} , we employ Tikhonov-regularized least-squares optimization. The objective function is defined as

$$\mathbf{u}^* = \arg \min_{\mathbf{u}} \|\mathbf{A}\mathbf{u} - \mathbf{b}\|_2^2 + \lambda \|\mathbf{L}\mathbf{u}\|_2^2, \quad (5)$$

where $\mathbf{u} = (\alpha, \kappa)$ denotes the control actions, with α and κ representing acceleration and curvature, respectively. The system matrix \mathbf{A} and input vector \mathbf{b} are derived from the kinematic model given in [11]. Given the initial velocity v_0 , and initial heading θ_0 , the control sequence \mathbf{u}^* is estimated and formatted into the final action string to be used as ground truth during training. During inference, the generated control actions are integrated to reconstruct the corresponding waypoints.

Action-based outputs are widely adopted in vision-language-action (VLA) models [34] by leveraging advanced generation techniques [35]. In this paper, both types of outputs are directly generated using the prediction model Driver-VLM. Table II summarizes the performance differences between the two output formulations. Waypoint-based prediction achieves lower short-term L2 error at the 1s, 2s, and 3s horizons. However, for long-term prediction, direct action prediction demonstrates superior performance in terms of overall average L2.

F. Ablation Studies

Table III presents the ablation studies of our framework, focusing primarily on the impact of different input configurations. All model variants include same reasoning inputs generated from Navi-VLM. From the results, we observe that incorporating high-level commands reduces the average L2 from 1.515 to 1.288 (-0.227). Since Driver-VLM is fundamentally a language model, explicitly providing intention information helps guide action prediction and improves planning performance. However, we find that incorporating image inputs does not significantly reduce average L2, which decreases only from 1.515 to 1.476 (-0.039) [36]. Despite the large number of image tokens, many may be redundant or contain limited task-relevant information, resulting in marginal performance gains. By combining reasoning, high-level commands, and image inputs, the final NaviDriveVLM model achieves a 6-second average L2 of 1.285, outperforming all other variants.

V. CONCLUSIONS

In this paper, we addressed a key challenge in VLM-based end-to-end autonomous driving: how to retain strong semantic reasoning while still achieving accurate motion planning. We introduced **NaviDriveVLM**, a decoupled Navigator–Driver framework in which large VLM models provides semantic guidance and small trainable VLM models predict future waypoints or actions. By treating reasoning as an explicit and interpretable intermediate representation between perception and planning, the proposed design preserves the

reasoning strengths of large models while allowing efficient adaptation for motion prediction. Experiments on the nuScenes benchmark show that the proposed decoupled design improves end-to-end motion planning over single VLM baselines, and our ablations further show that the Navigator’s reasoning contributes to these gains. Overall, these results support the idea that separating semantic reasoning from motion planning is a practical and effective direction for building autonomous driving systems that are both more interpretable and better aligned with planning performance.

REFERENCES

- [1] P. Taghavi, R. Langari, and G. Pandey, “Swinmtl: A shared architecture for simultaneous depth estimation and semantic segmentation from monocular camera images,” in *2024 IEEE/RSJ International Conference on Intelligent Robots and Systems (IROS)*. IEEE, 2024, pp. 4957–4964.
- [2] Y. Hu, J. Yang, L. Chen, K. Li, C. Sima, X. Zhu, S. Chai, S. Du, T. Lin, W. Wang, *et al.*, “Planning-oriented autonomous driving,” in *Proceedings of the IEEE/CVF conference on computer vision and pattern recognition*, 2023, pp. 17 853–17 862.
- [3] Z. Li, K. Li, S. Wang, S. Lan, Z. Yu, Y. Ji, Z. Li, Z. Zhu, J. Kautz, Z. Wu, *et al.*, “Hydra-mdp: End-to-end multimodal planning with multi-target hydra-distillation,” *arXiv preprint arXiv:2406.06978*, 2024.
- [4] J. Mao, J. Ye, Y. Qian, M. Pavone, and Y. Wang, “A language agent for autonomous driving,” *arXiv preprint arXiv:2311.10813*, 2023.
- [5] L. Chen, O. Sinavski, J. Hünemann, A. Karnsund, A. J. Willmott, D. Birch, D. Maund, and J. Shotton, “Driving with llms: Fusing object-level vector modality for explainable autonomous driving,” in *2024 IEEE International Conference on Robotics and Automation (ICRA)*. IEEE, 2024, pp. 14 093–14 100.
- [6] X. Huang, E. M. Wolff, P. Vernaza, T. Phan-Minh, H. Chen, D. S. Hayden, M. Edmonds, B. Pierce, X. Chen, P. E. Jacob, *et al.*, “Drivegpt: Scaling autoregressive behavior models for driving,” *arXiv preprint arXiv:2412.14415*, 2024.
- [7] X. Tian, J. Gu, B. Li, Y. Liu, Y. Wang, Z. Zhao, K. Zhan, P. Jia, X. Lang, and H. Zhao, “Drivevlm: The convergence of autonomous driving and large vision-language models,” *arXiv preprint arXiv:2402.12289*, 2024.
- [8] J.-J. Hwang, R. Xu, H. Lin, W.-C. Hung, J. Ji, K. Choi, D. Huang, T. He, P. Covington, B. Sapp, *et al.*, “Emma: End-to-end multimodal model for autonomous driving,” *arXiv preprint arXiv:2410.23262*, 2024.
- [9] X. Zhou, X. Han, F. Yang, Y. Ma, V. Tresp, and A. Knoll, “Open-drivevla: Towards end-to-end autonomous driving with large vision language action model,” *arXiv preprint arXiv:2503.23463*, 2025.
- [10] Z. Yang, Y. Chai, X. Jia, Q. Li, Y. Shao, X. Zhu, H. Su, and J. Yan, “Drivemoe: Mixture-of-experts for vision-language-action model in end-to-end autonomous driving,” *arXiv preprint arXiv:2505.16278*, 2025.
- [11] Y. Wang, W. Luo, J. Bai, Y. Cao, T. Che, K. Chen, Y. Chen, J. Diamond, Y. Ding, W. Ding, *et al.*, “Alpamayo-r1: Bridging reasoning and action prediction for generalizable autonomous driving in the long tail,” *arXiv preprint arXiv:2511.00088*, 2025.
- [12] Y. Ma, T. Wei, N. Zhong, J. Mei, T. Hu, L. Wen, X. Yang, B. Shi, and Y. Liu, “Leapvad: A leap in autonomous driving via cognitive perception and dual-process thinking,” *arXiv preprint arXiv:2501.08168*, 2025.
- [13] Z. Xu, Y. Bai, Y. Zhang, Z. Li, F. Xia, K.-Y. K. Wong, J. Wang, and H. Zhao, “Drivegpt4-v2: Harnessing large language model capabilities for enhanced closed-loop autonomous driving,” in *Proceedings of the Computer Vision and Pattern Recognition Conference*, 2025, pp. 17 261–17 270.
- [14] Y. Xu, Y. Hu, Z. Zhang, G. P. Meyer, S. K. Mustikovela, S. Srinivasa, E. M. Wolff, and X. Huang, “Vlm-ad: End-to-end autonomous driving through vision-language model supervision,” *arXiv preprint arXiv:2412.14446*, 2024.
- [15] D. Hegde, R. Yasarla, H. Cai, S. Han, A. Bhattacharyya, S. Mahajan, L. Liu, R. Garrepalli, V. M. Patel, and F. Porikli, “Distilling multimodal large language models for autonomous driving,” in *Proceedings of the Computer Vision and Pattern Recognition Conference*, 2025, pp. 27 575–27 585.
- [16] B. Feng, Z. Mei, B. Li, J. Ost, F. Ghilotti, R. Girgis, A. Majumdar, and F. Heide, “Verdi: Vlm-embedded reasoning for autonomous driving,” *arXiv preprint arXiv:2505.15925*, 2025.
- [17] W. Liu, P. Liu, and J. Ma, “Dsdrive: Distilling large language model for lightweight end-to-end autonomous driving with unified reasoning and planning,” *arXiv preprint arXiv:2505.05360*, 2025.
- [18] H. Caesar, V. Bankiti, A. H. Lang, S. Vora, V. E. Liong, Q. Xu, A. Krishnan, Y. Pan, G. Baldan, and O. Beijbom, “nuscenes: A multimodal dataset for autonomous driving,” *arXiv preprint arXiv:1903.11027*, 2019.
- [19] J. Mao, Y. Qian, J. Ye, H. Zhao, and Y. Wang, “Gpt-driver: Learning to drive with gpt,” *arXiv preprint arXiv:2310.01415*, 2023.
- [20] W. Wang, J. Xie, C. Hu, H. Zou, J. Fan, W. Tong, Y. Wen, S. Wu, H. Deng, Z. Li, *et al.*, “Drivemlm: Aligning multi-modal large language models with behavioral planning states for autonomous driving,” *arXiv preprint arXiv:2312.09245*, 2023.
- [21] H. Shao, Y. Hu, L. Wang, G. Song, S. L. Waslander, Y. Liu, and H. Li, “Lmdrive: Closed-loop end-to-end driving with large language models,” in *Proceedings of the IEEE/CVF conference on computer vision and pattern recognition*, 2024, pp. 15 120–15 130.
- [22] C. Sima, K. Renz, K. Chitta, L. Chen, H. Zhang, C. Xie, J. Beißwenger, P. Luo, A. Geiger, and H. Li, “Drivelm: Driving with graph visual question answering,” in *European conference on computer vision*. Springer, 2024, pp. 256–274.
- [23] M. Nie, R. Peng, C. Wang, X. Cai, J. Han, H. Xu, and L. Zhang, “Reason2drive: Towards interpretable and chain-based reasoning for autonomous driving,” in *European Conference on Computer Vision*. Springer, 2024, pp. 292–308.
- [24] J. Yuan, S. Sun, D. Omeiza, B. Zhao, P. Newman, L. Kunze, and M. Gadd, “Rag-driver: Generalisable driving explanations with retrieval-augmented in-context learning in multi-modal large language model,” *arXiv preprint arXiv:2402.10828*, 2024.
- [25] S. Xing, C. Qian, Y. Wang, H. Hua, K. Tian, Y. Zhou, and Z. Tu, “Openemma: Open-source multimodal model for end-to-end autonomous driving,” in *Proceedings of the Winter Conference on Applications of Computer Vision*, 2025, pp. 1001–1009.
- [26] H. Liu, C. Li, Q. Wu, and Y. J. Lee, “Visual instruction tuning,” *Advances in neural information processing systems*, vol. 36, pp. 34 892–34 916, 2023.
- [27] S. Hu, L. Chen, P. Wu, H. Li, J. Yan, and D. Tao, “St-p3: End-to-end vision-based autonomous driving via spatial-temporal feature learning,” in *European Conference on Computer Vision*. Springer, 2022, pp. 533–549.
- [28] W. Zheng, R. Song, X. Guo, C. Zhang, and L. Chen, “Genad: Generative end-to-end autonomous driving,” in *European Conference on Computer Vision*. Springer, 2024, pp. 87–104.
- [29] J.-T. Zhai, Z. Feng, J. Du, Y. Mao, J.-J. Liu, Z. Tan, Y. Zhang, X. Ye, and J. Wang, “Rethinking the open-loop evaluation of end-to-end autonomous driving in nuscenes,” *arXiv preprint arXiv:2305.10430*, 2023.
- [30] B. Jiang, S. Chen, Q. Xu, B. Liao, J. Chen, H. Zhou, Q. Zhang, W. Liu, C. Huang, and X. Wang, “Vad: Vectorized scene representation for efficient autonomous driving,” in *Proceedings of the IEEE/CVF International Conference on Computer Vision*, 2023, pp. 8340–8350.
- [31] Q. Team, “Qwen3 technical report,” 2025. [Online]. Available: <https://arxiv.org/abs/2505.09388>
- [32] I. Loshchilov and F. Hutter, “Decoupled weight decay regularization,” *arXiv preprint arXiv:1711.05101*, 2017.
- [33] E. J. Hu, Y. Shen, P. Wallis, Z. Allen-Zhu, Y. Li, S. Wang, L. Wang, W. Chen, *et al.*, “Lora: Low-rank adaptation of large language models.” *Iclr*, vol. 1, no. 2, p. 3, 2022.
- [34] K. Black, N. Brown, D. Driess, A. Esmail, M. Equi, C. Finn, N. Fusai, L. Groom, K. Hausman, B. Ichter, *et al.*, “ π_0 : A vision-language-action flow model for general robot control,” *arXiv preprint arXiv:2410.24164*, 2024.
- [35] Y. Lipman, R. T. Chen, H. Ben-Hamu, M. Nickel, and M. Le, “Flow matching for generative modeling,” *arXiv preprint arXiv:2210.02747*, 2022.
- [36] Z. Li, Z. Yu, S. Lan, J. Li, J. Kautz, T. Lu, and J. M. Alvarez, “Is ego status all you need for open-loop end-to-end autonomous driving?” in *Proceedings of the IEEE/CVF Conference on Computer Vision and Pattern Recognition*, 2024, pp. 14 864–14 873.